ACS SENSORS

pubs.acs.org/acssensors

Article

Tandem Quantification of Multiple Carbohydrates in Saliva Using Surface-Enhanced Raman Spectroscopy

Duo Lin, Shang-Wei Yang, Chang-Lin Hsieh, Keng-Jia Hsu, Tianxun Gong, Qiong Wu, Sufang Qiu,* Shangyuan Feng,* and Kien Voon Kong*

Cite This: *ACS Sens.* 2021, 6, 1240−1247

Read Online

ACCESS | Metrics & More | Article Recommendations | Supporting Information

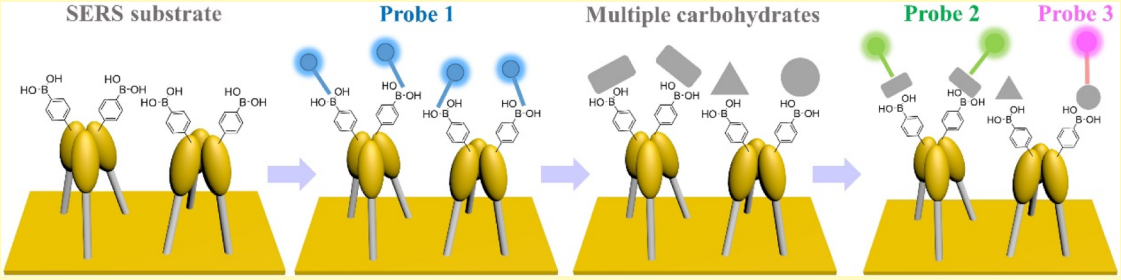

ABSTRACT: The detection of carbohydrates in human body fluids is critical for disease diagnosis and healthy monitoring. Despite recent advances in glucose sensing, multiplex detection of different carbohydrates within a single assay that is capable of efficiently providing richer health information remains challenging. Herein, we report a versatile surface-enhanced Raman spectroscopy-based platform for the quantitative detection of monosaccharides (glucose, fructose, and galactose) in one test using a displace-and-trap mechanism. Moreover, due to the use of multiple optical interference-free (1800−2200 cm^{-1}) signal-independent Raman probes, the detection range of this platform (0.125−7 mg/dL) perfectly covers physiological concentrations, enabling the quantitative detection of glucose and galactose in clinical human saliva samples. This work provides a noninvasive and high-efficiency potential tool for the screening of clinical diabetes and other carbohydrate-related diseases.

KEYWORDS: *surface-enhanced Raman spectroscopy, biosensor, carbohydrates, metal carbonyl, bioorganometallic chemistry*

Downloaded via BUTLER UNIV on May 16, 2021 at 10:56:36 (UTC).
See https://pubs.acs.org/sharingguidelines for options on how to legitimately share published articles.

An unprecedented increase in the number of patients with diabetes mellitus and its complicating factors has contributed tremendously to the burden of mortality and disability worldwide. According to International Diabetes Federation (IDF) data, an estimated 642 million people will suffer from this metabolic disorder by the year 2040, resulting from the increase in an energy-dense diet and the aging population.[1,2] The level of glucose in biofluids has been acknowledged as the most important index for both the diagnosis and management of diabetes.

Other metabolic diseases including fructose malabsorption, fructosemia, and galactosemia are clinically important. This is because elevated level of fructose and galactose can lead to serious complications such as liver and kidney failure.[3−5] Therefore, routine fructose and galactose monitoring is important for galactosemia or fructosemia patients. The current clinical test for fructosemia is based on the detection of hydrogen and methane gas in breath (bacteria in colon will digest fructose and release hydrogen and methane gases). For galactosemia test, it is done with blood detection. These tests are extremely challenging due to the problems of the inherently poor reproducibility and high false positive rate.[6,7] Due to their great importance in disease diagnosis, the development of reliable and fast alternative detection methods for fructose and galactose continues to be of interest.

Surface-enhanced Raman spectroscopy (SERS) based on inelastic scattering processes is a powerful analytical technology in biomedical research. With distinct enhancement effects (electromagnetic and chemical enhancement) at the nanoscale, SERS is capable of achieving single-molecule detection and has thus been widely applied to detect various biosamples, ranging from small molecules to proteins, cells, body fluids, and tissues.[8−14] All of these features suggest that SERS is an ideal tool for practical detection in body fluids. For example, Van Duyne's group first presented a glucose biosensor based on SERS. By partitioning glucose into an alkanethiol monolayer adsorbed on a silver surface, they successfully circumvented the adsorption problem and achieved quantitative glucose detection in a clinically relevant concentration range.[15] To

Received: December 3, 2020
Accepted: January 25, 2021
Published: February 9, 2021

© 2021 American Chemical Society

https://dx.doi.org/10.1021/acssensors.0c02533
ACS Sens. 2021, 6, 1240−1247

further increase the selectivity of glucose sensing, the same group designed a gold film over a nanosphere substrate functionalized with bisboronic acid receptors for direct glucose detection by SERS.[16] Although promising, most glucose sensors based on SERS suffer from interference from biomolecules due to the featured SERS peaks of glucose in the fingerprint region. In the context of this situation, our group employed a metal carbonyl SERS probe with silent Raman signals (1800−2200 cm^{-1}) for highly sensitive and selective glucose detection.[17] Recently, new challenges in glucose detection in saliva using SERS have emerged. However, to date, a versatile SERS-based platform for the detection of salivary glucose, galactose, and fructose has not been reported.

Multiplexed detection of monosaccharides would allow clinicians to monitor and establish a correlation among them, thus achieving precise diagnosis. The absence of such a platform is due to the lack of a system that can optically detect these three carbohydrates within a single sensor. Herein, we report a SERS method for glucose, galactose, and fructose detection within a single chip involving a facile tandem reaction of the three carbohydrates with boronic acid probes. With the merits of the selectivity effect between the metal carbonyl conjugated boronic probe and the fluorinated boronic acid probe, the assay exhibits high response rate to glucose and galactose. With a combination of a displacement probe, fructose is detected as well. The levels of glucose and galactose in clinical human saliva samples are essentially detected and quantified.

EXPERIMENTAL SECTION

SERS Measurement. A microscopic Raman instrument (Renishaw) with a 785 nm laser, a 50× objective lens, and a Peltier cooled charge-coupled device was used for Raman spectral measurement.

A silicon wafer with a Raman peak at 520 cm^{-1} was used for signal calibration before each SERS measurement. After that, each spectrum was obtained with 10 s acquisition time and then underwent the process of baseline correction using the software (WiRE 4.3) with a curve fitting and polynomial multipoint fitting function. The final intensities of Raman peaks were used for spectral analysis, such as quantitative analysis.

Fabrication of Nanopillar Substrate. A four inch p-type single side polished ⟨100⟩ wafer was used. The wafer was first washed with buffered oxide etch ($NH_4F/HF/H_2O$) and then placed for 5 min in an oven at 120 °C to remove water from the surface. Etching is conducted in a reactive ion etching system (RIE-10N, SAMCO). After that, the wafer was processed to an O_2 plasma cleaner under 2.0 × 10^{-1} Torr vacuum (PDC-001 cleaner from Harrick Plasma). In order to totally remove the decomposition products and etchant gas residuals, the wafer was exposed to argon plasma for 1 min. For the E-beam evaporation process, FULINTEC E-GUN was used. The rate evaporation of chromium was 0.1 Å/s, and the thickness of chromium on wafer was 0.17 nm. Gold was subsequently deposited on the substrate with the rate of evaporation at 1.0 Å/s and the thickness was 180 nm. The wafer was then processed for precision dicing with the size of 3 mm × 3 mm (DS-150 II from EVERPRECISION TECH).

Immobilization of 4-Mercaptophenylboronic Acid on Nanopillar Substrate. 4-Mercaptophenylboronic acid (MPBA, 1.54 mg) was dissolved in 10 mL of ethanol. The fabricated nanopillar substrate was then incubated in 2 mL of MPBA solution for 2 h. The substrate was washed with ethanol three times and blow-dried under argon flow.

Immobilization of 3,4-Dihydroxybenzonitrile (DBN−C≡N) on MPBA. 3,4-Dihydroxybenzonitrile (13.5 mg) was dissolved in 10 mL of a pH 10 solution adjusted by sodium hydroxide. The substrate coated with MPBA was soaked into 2 mL of 3,4-dihydroxybenzonitrile for 1 h. The substrate was blow-dried under argon flow.

Binding of Glucose, Fructose, and Galactose. The substrate coated with MPBA−DBN−C≡N was incubated with 1 mM of glucose, fructose, and galactose in deionized water. The pH was adjusted to pH 10. After 2 h, the substrate was washed with water three times and blow-dried under argon flow.

Synthesis of Triosmium Carbonyl Cluster−Boronic Acid Conjugates (Os−BA−C≡O). $Os_3(CO)_{10}(NCCH_3)_2$ (26 mg, 0.028 mmol) and MPBA (5 mg, 0.034 mmol) were dissolved in tetrahydrofuran (6 mL), followed by stirring at room temperature overnight. Under *vacuo*, the solvent was removed and thin-layer chromatography was employed to purify the residue using ethyl acetate/hexane (1:1, v/v) as eluant to yield one major yellow band as cluster Os−BA. Yield: 22 mg (69%); R_f = 0.37; IR (DCM, cm^{-1}) ν_{CO}: 2110w, 2069s, 2060m, 2023s, 2001m, 1987w. ^1H NMR (400 MHz, $(CD_3)_2CO$): δ 7.62 (2H, d, Ar), 7.39 (2H, d, Ar), 7.32 (2H, s, $B(OH)_2$).

Detection of Glucose with Os−BA−C≡O. Os−BA−C≡O (1 mM) at pH 10 was prepared. The resulted solution was then added to the substrate MPBA−glucose. After 2 h, the substrate was washed with water three times and blow-dried under argon flow.

Detection of Galactose with 3-Fluorophenylboronic Acid (F−BA−C≡N). 3-Fluorophenylboronic acid (13.9 mg) was dissolved in 10 mL of a pH 10 solution. The substrate with MPBA−galactose was soaked into 2 mL of 3-fluorophenylboronic acid solution for 2 h. The substrate was blow-dried under argon flow.

Calculation of the Binding Constant. The apparent 2:1 binding constant (K_a) with sugars (glucose and galactose) in the presence of Os−BA−C≡O or F−BA−C≡N was determined from the changes in the SERS spectra. On the assumption that the SERS change is only induced by the formation of a 2:1 complex (bidentate complex) among MPBA, sugar, and Os−BA−C≡O or F−BA−C≡N, the binding constant can be defined as shown in Figure S4.

Electromagnetic Simulation. The high mesh density simulations for plasmonic properties of gold nanoparticles were performed using commercial software (COMSOL Multiphysics 3.5a version) with an rf extended module. In the draw mode of the Cartesian coordinate system, the particle size and three-dimensional shape can be drawn, and boundary conditions and perfectly matched layer can be also defined. The simulation process for a single nanoparticle lasted for 4 h. A Lenovo desktop equipped with Intel Core 2 Quad CPU Q9650 at 3.00 GHz and 8 GB RAM, as well as a 64-bit Windows 7 Professional operating system, was employed for the above simulations.

Patient Sample Collection. Saliva samples were collected from unstimulated participants (50 years old, Fujian Cancer Hospital) in order to show their real metabolic conditions, which would improve the test accuracy. Patients with other diseases and pregnant women were excluded from this study. The approval (K201401) from Fujian Cancer Hospital ethics committee was obtained prior to this research, and informed written consent was obtained from all the subjects taking part in the study. After 8 h of overnight fasting, the saliva samples were obtained from the study subjects after the mouth rinsing between 6:30 and 7:30 a.m. During the collection process, each saliva sample was naturally drained into the tube within 5 min. Following saliva collection, 5 mL of blood from the same subject was collected using a sterile test tube. Each saliva and blood sample (1 mL) was respectively centrifuged using an ultracentrifuge to separate at 3000 rpm for 20 min, and clear supernatants were obtained. Three independent experiments were performed for each sample.

Statistical Analysis. Means and standard deviations were calculated for the individual groups. The database of testing results was constructed using Microsoft Excel to aid statistical analysis. Student's *t*-test was used to evaluate the significance of differences between the two study groups. Probabilities of less than 0.05 were accepted as significant.

Continuous Monitoring of the Biosensors. In the absence of target, the SERS intensities of biosensors were monitored for 60 min at 0.5 min intervals using wavelengths of 785 nm. Then, diol stock

https://dx.doi.org/10.1021/acssensors.0c02533
ACS Sens. 2021, 6, 1240−1247

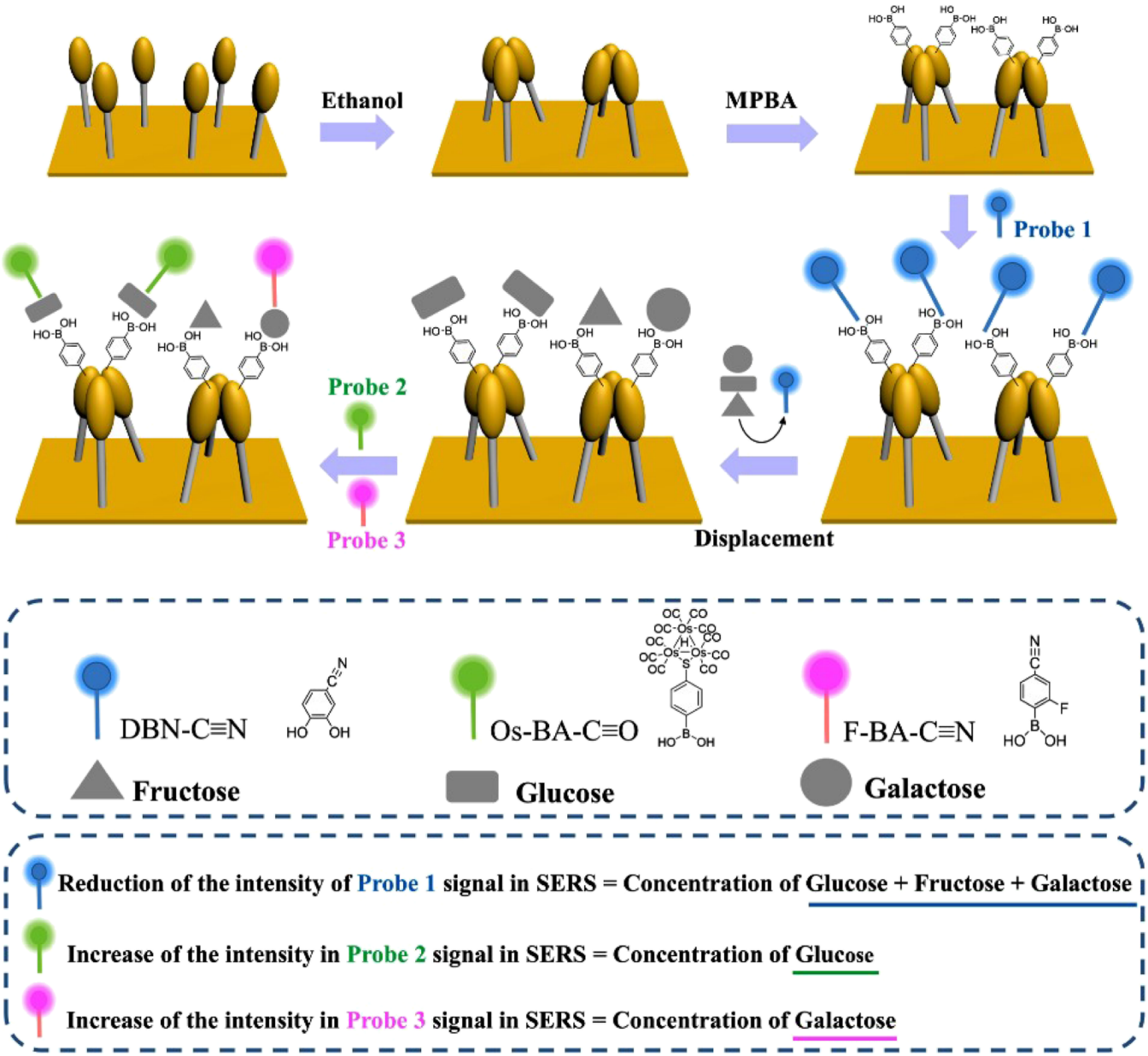

Figure 1. Schematic representation of the detection mechanism of glucose, fructose, and galactose *via* multiple optical interference-free SERS probes.

solutions in varying concentrations were added to the biosensors, followed by SERS monitoring for another 60 min at 0.5 min intervals. The percent binding of diol was calculated. This relatively long incubation time was employed to ensure that the solutions reached equilibrium. The sensor reached equilibrium after 1 h. Upon exposure to glucose solution, the binding equilibrium reached to saturation in less than 60 min.

RESULTS AND DISCUSSION

Principle of Assay. This assay relies on the abilities of glucose and galactose to form a bidentate glucose and galactose boronic complex and fructose to form a boronic monodentate complex (Figure 1).[18−22] Three carbohydrate probes are used. The primary probe 3,4-dihydroxybenzonitrile (DBN−C≡N; a displacement probe with a nitrile group signal at 2226 cm^{-1}) is weakly bound to the MPBA capture receptor and can detect the total concentration of the three monosaccharides. All the three monosaccharides are first captured by MPBA through the displacement of DBN−C≡N, followed by subsequent strong binding of the MPBA−triosmium carbonyl cluster (Os−BA−C≡O; a secondary probe with a carbon monoxide signal at 2111 cm^{-1}) to glucose and 4-cyano-3-fluorophenylboronic acid (F−BA−C≡N; a secondary probe with a nitrile group signal at 2235 cm^{-1}) to galactose (Figure S1). Os−BA−C≡O is often stable to both air and moisture (Figure S2).[23] We previously demonstrated its ability to bind glucose. It is thus possible to quantify the total saccharides (glucose + fructose + galactose) in samples with the displacement reaction of DBN−C≡N. Then, we can selectively quantify the concentrations of glucose and galactose *via* the C≡O and C≡N stretching vibrations of Os−BA−C≡O and F−BA−C≡N, respectively. The subsequent signal subtraction of F−BA−C≡N from DBN−C≡N plus Os−BA−C≡O can be used to obtain the concentration of fructose.

https://dx.doi.org/10.1021/acssensors.0c02533
ACS Sens. 2021, 6, 1240−1247

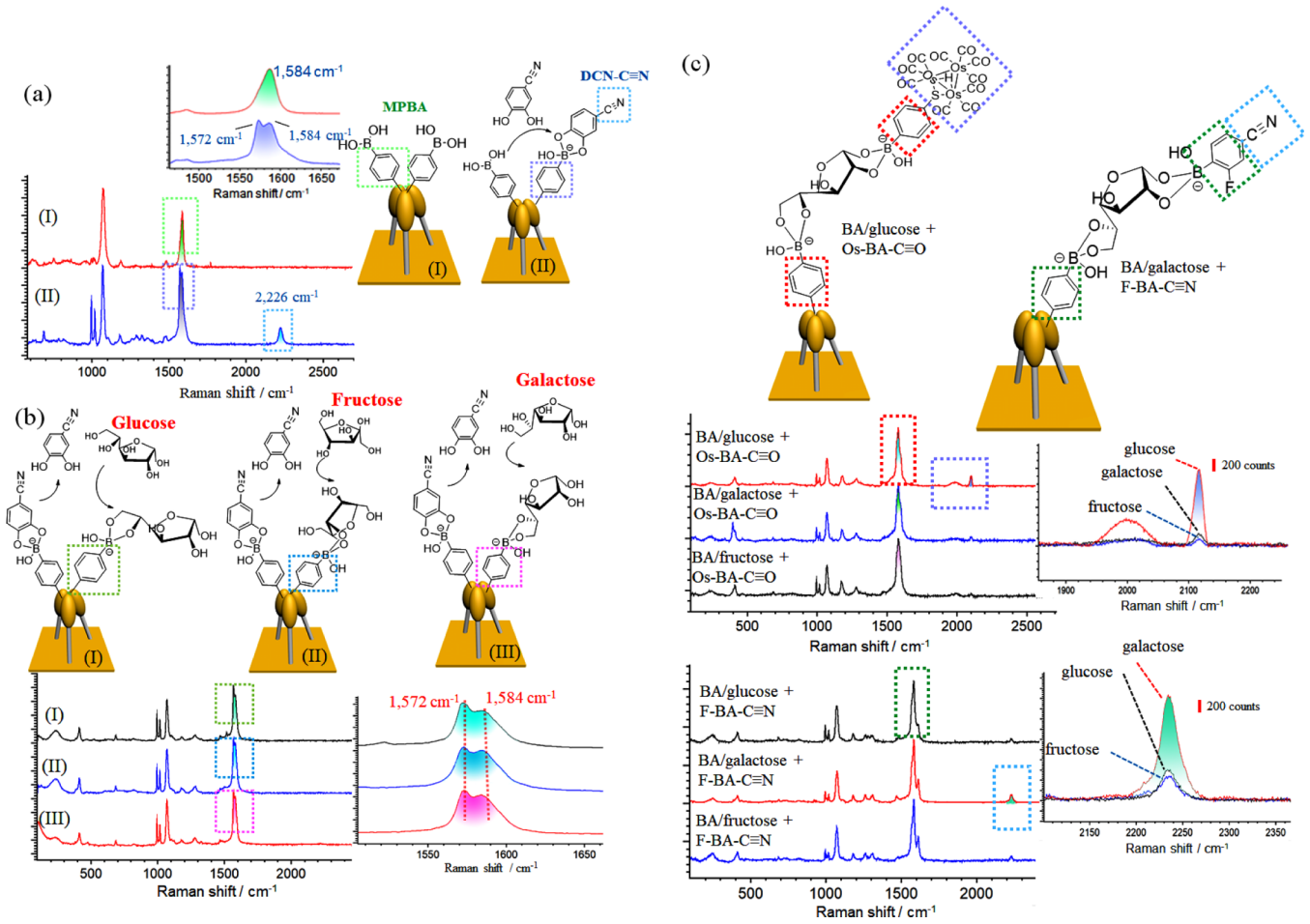

Figure 2. (a) SERS spectra of DBN−C≡N binding MPBA exhibiting a new detectable peak at 2226 cm^{-1} and inducing distortion of the benzene ring of boronic acid. (b) SERS spectra of MPBA−DBN−C≡N after incubation with glucose, galactose, and fructose binding demonstrating a disappearance of the peak associated with DBN−C≡N. (c) Os−BA−C≡O and F−BA−C≡N exhibit high-intensity peaks in the presence of glucose and galactose, respectively.

Optical Properties of Nanopillar Substrate. Free-standing nanopillars coated with gold can act as effective SERS substrates.[24] These are in-house fabricated substrates comprising a multiple nanopillar structure formed by chemical etching and the deposition of gold *via* electron beam evaporation (Figure S3). The localized surface plasmon resonance (LSPR) resonance peak position of nanopillar is ∼700 nm. MPBA is immobilized onto the nanopillar *via* a thiol−gold reaction and then modified with DBN−C≡N, which can be confirmed by the excellent enhancement of the Raman signal at 2226 cm^{-1} (Figure 2a). The relative intensities of the peaks at 1572 and 1584 cm^{-1} change that is attributed to the symmetric ring mode and non-totally symmetric ring mode of the MPBA benzene ring are due to DBN−C≡N binding to the boronic acid moiety, which breaks the symmetry of the probe.[25]

MPBA−DBN−C≡N can then be incubated with a 1 mM solution of glucose, fructose, and galactose. While a significant reduction in the DBN−C≡N signal (2226 cm^{-1}) is observed (Figure 2b), the distortion of the boronic acid moiety symmetry is still noticeable (1572 and 1584 cm^{-1}). This indicates that the DNB−C≡N moiety is displaced by glucose, fructose, and galactose.[25]

Subsequent incubation with Os−BA−C≡O under basic conditions results in a strong detectable CO signal (2111 cm^{-1}) for MPBA−glucose (Figure 2c). The pH profiles of the Os−BA−C≡O complexes with glucose show that the peak at 2111 cm^{-1} increased under basic conditions (Figure 3a). Given the geometry of the MPBA−glucose−Os−BA−C≡O sandwich and considering that SERS enhancement can occur in the nanometer range, C≡O can be observed within the SERS enhancement range if Os−BA−C≡O binds to MPBA−glucose (Figure 3b,c). We estimated a molecular distance of glucose of approximately 10 Å, and the two boronic acid plus osmium clusters are still within the detection range (Figure 3d,e). The pK_a value of Os−BA−C≡O with glucose is 10.85. On the other hand, the substrate treated with fructose and galactose shows a very modest CO stretching peak (Figure 2c).

In studying the reaction kinetics, significant SERS intensity changes were observed upon mixing of the various sugars (Figure 3g). One can quickly see that all reactions reach equilibria within 60 min. The reaction between glucose and MPBA−DBN−C≡N substrate reached equilibrium within 60 min. Thus, the experiment was always equilibrated in the sample solution for 60 min before SERS measurement was carried out. Our results are in line with other boronic acid binding events.[26,27] It is generally believed that boronic acid−diol binding is rapidly reaching equilibrium. Thus, 60 min incubation time was employed to ensure that the solutions reached equilibrium.

https://dx.doi.org/10.1021/acssensors.0c02533
ACS Sens. 2021, 6, 1240−1247

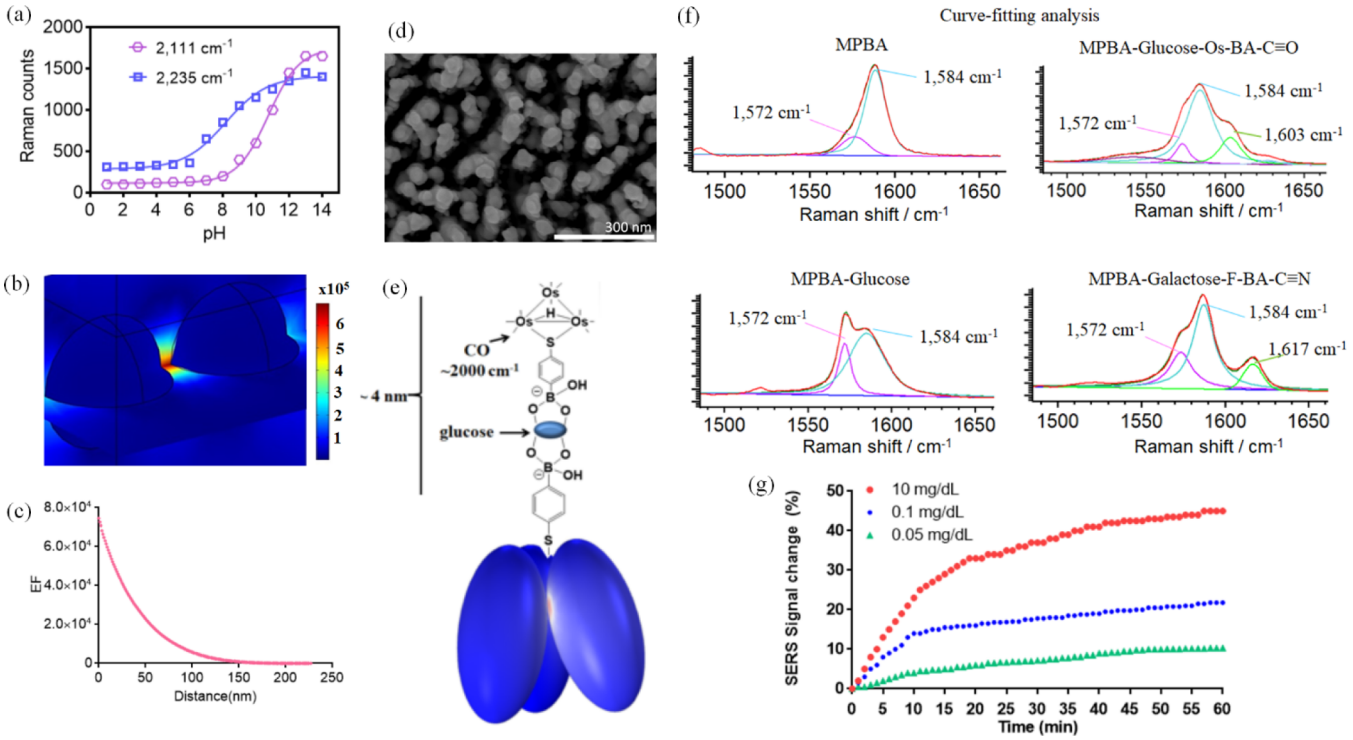

Figure 3. (a) pH profiles of Os−BA−C≡O and F−BA−C≡N. (b) Gold nanopillars with simulated electric field distribution ($|E|/|E_0|$) around the gold nanopillars. (c) Calculated Raman enhancement factor for gold nanopillars with different distances. (d) Scanning electron microscopy image of the gold nanopillar substrate. (e) Schematic representation of the geometry of MPBA−glucose−Os−BA−C≡O within the nanometer range of SERS enhancement. (f) Curve-fitting analysis demonstrates the changes in the stretching frequency of the benzene ring. (g) Incubation of glucose with the MPBA−DBN−C≡N substrate.

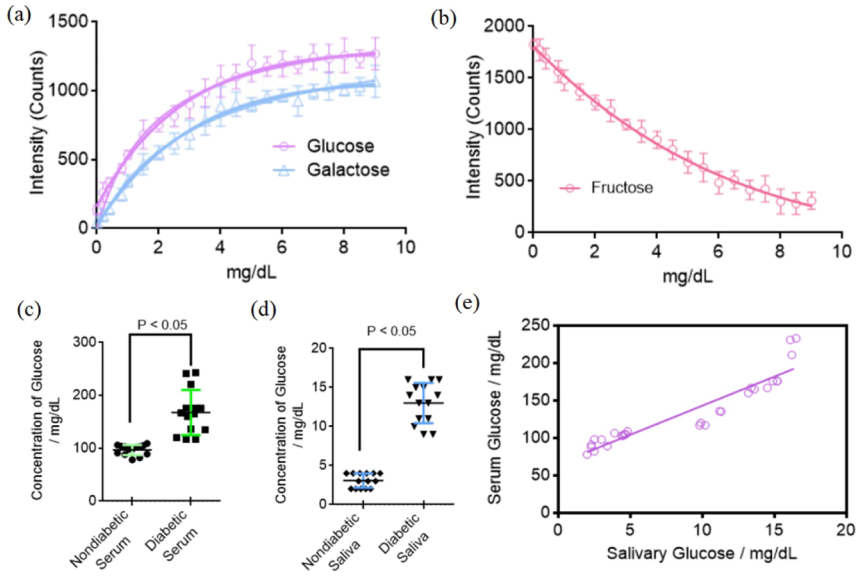

Figure 4. (a) Concentration plots for glucose and galactose detection. (b) Incubation of fructose with the MPBA−DBN−C≡N substrate. Comparison of glucose levels in (c) serum and (d) saliva in nondiabetic and diabetic patients. (e) Correlation between salivary and blood glucose levels in both diabetic patients group and control group (each value is the mean of triplicate assays).

Multiplex Detection of Different Carbohydrates. The quantification capabilities of galactose can be determined using the Raman signature of F−BA−C≡N at 2235 cm^{-1}. The pH profile of F−BA−C≡N was also measured (Figure 3a). The pK_a value of F−BA−C≡N is 8.46. The lower pK_a value of F−BA−C≡N is due to the electron-withdrawing effect of the fluorine moiety of the boronic acid probe. Furthermore, the sugar recognition ability of F−BA−C≡N was determined. The results show that the signals at 2111 and 2235 cm^{-1} increase with increasing glucose and galactose concentrations, respectively (Figure 2c). Thus, it is obvious that the formation of the complex of boronic acids with glucose or galactose occurred. The calculated binding constants of Os−BA−C≡O

https://dx.doi.org/10.1021/acssensors.0c02533
ACS Sens. 2021, 6, 1240−1247

and F−BA−C≡N to glucose and galactose are found to be 1100 and 1000 M^{-1}, respectively.

The binding of Os−BA−C≡O to MPBA−glucose and F−BA−C≡N to MPBA−galactose results in further distortion of the band from the benzene ring of the boronic acid moieties. As demonstrated by curve-fitting analysis, the symmetric ring mode and non-totally symmetric ring mode of the MPBA benzene ring remain (Figure 3f). The addition of the boronic acid benzene ring of Os−BA−C≡O contributes to the shoulder of the peak at 1603 cm^{-1} and an increase in the intensity of the peak at 1584 cm^{-1}. Likewise, the binding of F−BA−C≡N to MPBA−galactose contributes to the shoulder of the peak at 1617 cm^{-1} and an increase in the intensity of the peak at 1584 cm^{-1}. The difference in the binding affinities of Os−BA−C≡O and F−BA−C≡N to glucose and galactose can discriminate glucose and galactose by the C≡O and C≡N bands, and two concentration dependence curves are obtained (Figure 4a). The non-specific binding of DBN−C≡N, F−BA−C≡N, and Os−BA−C≡O was tested. It showed no non-specific binding to the nanopillars substrate.

The intensity of the sharp peak at 2111 cm^{-1} changes as an indicator of concentration after incubation with different concentrations of glucose, whereas the peak at 2235 cm^{-1} corresponds well with the concentration of galactose; the limits of detection are estimated to be 0.125 mg/dL for glucose and 0.259 mg/dL for galactose (Figures S5 and S6). Both detection ranges cover physiological concentrations (nondiabetic patients: ≤5 mg/dL and diabetic patients: ≥5 mg/dL).[28,29]

The concentration of fructose in solution was calculated using the DBN−C≡N (2226 cm^{-1}) peak from the subtraction of the glucose and galactose sample addition to the nanopillar. We also tested the displacement ability of DBN−C≡N by fructose in the absence of glucose and galactose. As shown in Figure 4b, the disappearance of the DBN−C≡N signal is well correlated with the concentration of fructose. This detection limit compares very well with a similar glucose and fructose assay and has a detection limit of 1.35 mg/dL. The selectivity is due to the use of the higher binding affinity of fructose to monoboronic acids and glucose and galactose to form bisboronic acid adducts.[30] Therefore, both glucose and galactose interacted with MPBA−DBN−C≡N on the nanopillar, but there was preferential binding of Os−BA−C≡O and F−BA−C≡N with the surface-bound glucose and galactose, respectively.[31,32]

Detection of Salivary Carbohydrates. Glucose monitoring for diabetes is usually carried out on blood samples. Salivary glucose detection is a useful non-invasive screening method. Since saliva collection is safe and convenient, further research should be conducted to evaluate the feasibility of saliva as an alternative diagnostic fluid.[33−37] Saliva that can provide valuable molecular information is a substitute, alternative, or complement when the blood glucose test is not affordable, accessible, or desirable in some clinical cases.

To access the potential clinical applications of the proposed sensing method, we collected saliva samples from patients with diabetes and healthy volunteers as controls as summarized in Table S1. A total of 28 samples were collected. Saliva samples were collected from each unstimulated participant, which revealed the metabolic conditions of the real participants. This led to an increase in test accuracy. This is because unstimulated saliva is the amount of saliva secreted by the major and minor glands. Therefore, there is no detectable fructose concentration in the saliva samples. The results show that tandem detection using boronic acid probes is significantly outperforming the commercial glucose meter (limit of detection of glucose meter is 100 mg/dL). Moreover, the tandem assay manifests a good galactose detection in saliva samples. The glucose concentration average is 3.53 ± 1.1 mg/dL (n = 14) (serum glucose = 96.5 mg/dL) in unstimulated control saliva, which is distinct from the glucose concentration average of 13.41 ± 2.46 mg/dL (n = 14) in the unstimulated saliva of diabetic patients [serum glucose = 167.86 mg/dL (n = 14)] (Figures 4c,d and S7).

The differences in salivary glucose and serum glucose for normal and diabetic patients were also analyzed with a t-test and are statistically significant ($P < 0.05$). Previous studies have reported increases in salivary glucose levels in patients with diabetes mellitus compared to nondiabetic patients.[38,39] In this study, there appears a positive correlation between salivary and serum glucose in both diabetic patient group and control group (Figure 4e). All of these correlations are statistically significant. Therefore, the salivary glucose value can well indicate the concentration of serum glucose in diabetic patients. We found that patients with serum glucose value above 167.86 mg/dL showed an average salivary glucose value of 13.41 mg/dL. On this occasion, we can conclude that patients with salivary glucose value above 13.41 mg/dL would likely suggest a serum glucose value above 167.86 mg/dL. We also estimated the galactose levels in patients with diabetes (Table S1). The galactose concentration is higher than the glucose concentration, which is in line with previously reported findings.[40] However, we could not establish a correlation between salivary galactose and serum glucose levels at this stage.

A comparison with other techniques was made. The surface plasmon resonance (SPR) technique is used to detect the shift of SPR peak resulted in H_2O_2 produced by glucoxidase. However, the stability of enzyme during storage at room temperature is a critical problem.[41] Although the fluorescence detection technique is very sensitive for low glucose concentration, it suffers from photobleaching and underestimation of glucose concentration due to variation in the excitation source.[42] To resolve this problem, other fluorescence materials were developed for glucose sensing such as Qdot.[43] However, it is required to couple with glucoxidase to produce a fluorescence signal (experiment time: 45 min). While a two-dimensional (2D) photonic sensor, where it detects the change in diffraction wavelength, has lower limit of detection,[27] our sensor has the potential to simultaneously detect multiple biomolecules. Our sensor possesses similar experiment time with SPR technique (experiment time: 120 min) and 2D photonic sensor (experiment time: 120 min). While the Qdot/silver nanoparticle method has shorter reaction time, it can potentially suffer from background interference due to fluorescence emission by serum.[44]

CONCLUSIONS

A tandem detection of multiple monosaccharides is rationally designed as a promising SERS sensor. The details chemical binding analysis revealed that metal carbonyl conjugated boronic acid probe, fluorinated boronic acid probe, and the displacement probe can achieve high response rate for the quantitative detection of monosaccharides. The detection range of carbohydrates is 0.125−7 mg/dL, which covers the physiological concentrations, thus enabling us to quantitatively detect glucose and galactose in clinical human saliva samples.

https://dx.doi.org/10.1021/acssensors.0c02533
ACS Sens. 2021, 6, 1240−1247

The proof-of-concept study on SERS detection of multiple carbohydrates in human body fluids would contribute significant advances in carbohydrate detection field and has great potential applications for the screening of clinical diabetes and other carbohydrate-related diseases with high efficiency.

■ ASSOCIATED CONTENT

Supporting Information

The Supporting Information is available free of charge at https://pubs.acs.org/doi/10.1021/acssensors.0c02533.

SERS spectrum of DBN−C≡N, Os−BA−C≡O, and F−BA−C≡N; ^{1}H NMR spectrum, IR spectrum, and mass spectrum of Os−BA−C≡O; fabricated gold nanopillar substrate; LSPR resonance peak position of nanopillar; determination of binding constant; relationship between SERS signals and glucose concentration; relationship between SERS signals and galactose concentration; Student's *t*-test analysis; and detection of monosaccharides with tandem sensing, commercial glucose meter, and assay kits (PDF)

■ AUTHOR INFORMATION

Corresponding Authors

Sufang Qiu − *Department of Radiation Oncology, Fujian Provincial Key Laboratory of Translational Cancer Medicine, Fujian Medical University Cancer Hospital & Fujian Cancer Hospital, Fuzhou 350014, China*; Email: sfqiu@126.com

Shangyuan Feng − *Key Laboratory of OptoElectronic Science and Technology for Medicine, Ministry of Education, Fujian Provincial Key Laboratory for Photonics Technology, Digital Fujian Internet-of-Things Laboratory of Environment Monitoring, Fujian Normal University, Fuzhou 350007, China*; Email: syfeng@fjnu.edu.cn

Kien Voon Kong − *Department of Chemistry, National Taiwan University, Taipei 10617, Taiwan*; orcid.org/0000-0002-5910-6497; Email: kvkong@ntu.edu.tw

Authors

Duo Lin − *Key Laboratory of OptoElectronic Science and Technology for Medicine, Ministry of Education, Fujian Provincial Key Laboratory for Photonics Technology, Digital Fujian Internet-of-Things Laboratory of Environment Monitoring, Fujian Normal University, Fuzhou 350007, China*; orcid.org/0000-0001-6959-5995

Shang-Wei Yang − *Department of Chemistry, National Taiwan University, Taipei 10617, Taiwan*

Chang-Lin Hsieh − *Department of Chemistry, National Taiwan University, Taipei 10617, Taiwan*

Keng-Jia Hsu − *Department of Chemistry, National Taiwan University, Taipei 10617, Taiwan*

Tianxun Gong − *State Key Laboratory of Electronic Thin Films and Integrated Devices, School of Electronic Science and Engineering (National Exemplary School of Microelectronics), University of Electronic Science and Technology of China, Chengdu 610054, China*

Qiong Wu − *Key Laboratory of OptoElectronic Science and Technology for Medicine, Ministry of Education, Fujian Provincial Key Laboratory for Photonics Technology, Digital Fujian Internet-of-Things Laboratory of Environment Monitoring, Fujian Normal University, Fuzhou 350007, China*

Complete contact information is available at: https://pubs.acs.org/10.1021/acssensors.0c02533

Notes

The authors declare no competing financial interest.

■ ACKNOWLEDGMENTS

This work was supported by financial support from the Ministry of Science and Technology (MOST), Taiwan (grant no. 108-2113-M-002-005-MY2), and the Faculty of Science, National Taiwan University (grant nos. 110L7821 and 109L4000). D.L. and S.F. acknowledge the support from the National Natural Science Foundation of China (nos. 11974077 and 61975031) and the Innovation Team Development Plan by the Ministry of Education of China (no. IRT15R10). The special funds of the Central Government Guiding Local Science and Technology Development (no. 2020L3008) were also acknowledged.

■ REFERENCES

(1) Chatterjee, S.; Khunti, K.; Davies, M. J. Type 2 diabetes. *Lancet* **2017**, *389*, 2239−2251.

(2) Zheng, Y.; Ley, S. H.; Hu, F. B. Global aetiology and epidemiology of type 2 diabetes mellitus and its complications. *Nat. Rev. Endocrinol.* **2018**, *14*, 88−98.

(3) Uusitupa, M. I. Fructose in the diabetic diet. *Am. J. Clin. Nutr.* **1994**, *59*, 753S−757S.

(4) Kawasaki, T.; Akanuma, H.; Yamanouchi, T. Increased Fructose Concentrations in Blood and Urine in Patients With Diabetes. *Diabetes Care* **2002**, *25*, 353−357.

(5) Hannou, S. A.; Haslam, D. E.; McKeown, N. M.; Herman, M. A. Fructose metabolism and metabolic disease. *J. Clin. Invest.* **2018**, *128*, 545−555.

(6) Yao, C. K.; Tuck, C. J. The clinical value of breath hydrogen testing. *J. Gastroenterol. Hepatol.* **2017**, *32*, 20−22.

(7) Kwon, C.; Farrell, P. M. The Magnitude and Challenge of False-Positive Newborn Screening Test Results. *Arch. Pediatr. Adolesc. Med.* **2000**, *154*, 714−718.

(8) Zhang, Y.; Jimenez de Aberasturi, D.; Henriksen-Lacey, M.; Langer, J.; Liz-Marzán, L. M. Live-Cell Surface-Enhanced Raman Spectroscopy Imaging of Intracellular pH: From Two Dimensions to Three Dimensions. *ACS Sens.* **2020**, *5*, 3194−3206.

(9) Zhang, W.; Jiang, L.; Diefenbach, R. J.; Campbell, D. H.; Walsh, B. J.; Packer, N. H.; Wang, Y. Enabling Sensitive Phenotypic Profiling of Cancer-Derived Small Extracellular Vesicles Using Surface-Enhanced Raman Spectroscopy Nanotags. *ACS Sens.* **2020**, *5*, 764−771.

(10) Sun, D.; Xu, W.; Liang, C.; Shi, W.; Xu, S. Smart Surface-Enhanced Resonance Raman Scattering Nanoprobe for Monitoring Cellular Alkaline Phosphatase Activity during Osteogenic Differentiation. *ACS Sens.* **2020**, *5*, 1758−1767.

(11) Wang, Z.; Zong, S.; Wu, L.; Zhu, D.; Cui, Y. SERS-Activated Platforms for Immunoassay: Probes, Encoding Methods, and Applications. *Chem. Rev.* **2017**, *117*, 7910.

(12) Kim, N.; Thomas, M. R.; Bergholt, M. S.; Pence, I. J.; Seong, H.; Charchar, P.; Todorova, N.; Nagelkerke, A.; Belessiotis-Richards, A.; Payne, D. J.; Gelmi, A.; Yarovsky, I.; Stevens, M. M. Surface enhanced Raman scattering artificial nose for high dimensionality fingerprinting. *Nat. Commun.* **2020**, *11*, 207.

(13) Chen, W.; Kang, Y.; Zhang, H.; Huang, T.; Tao, X.; Lu, A.; Du, Y. One-pot synthesis of silver colloid with body-heat for surface-enhanced Raman spectroscopy detections. *Chin. Chem. Lett.* **2019**, *30*, 1027−1030.

(14) Li, S.; Xu, J.; Wang, S.; Xia, X.; Chen, L.; Chen, Z. Versatile metal graphitic nanocapsules for SERS bioanalysis. *Chin. Chem. Lett.* **2019**, *30*, 1581−1592.

(15) Shafer-Peltier, K. E.; Haynes, C. L.; Glucksberg, M. R.; Van Duyne, R. P. Toward a Glucose Biosensor Based on Surface-Enhanced Raman Scattering. *J. Am. Chem. Soc.* **2003**, *125*, 588−593.
(16) Sharma, B.; Bugga, P.; Madison, L. R.; Henry, A. I.; Blaber, M. G.; Greeneltch, N. G.; Chiang, N.; Mrksich, M.; Schatz, G. C.; Van Duyne, R. P. Bisboronic Acids for Selective, Physiologically Relevant Direct Glucose Sensing with Surface-Enhanced Raman Spectroscopy. *J. Am. Chem. Soc.* **2016**, *138*, 13952−13959.
(17) Kong, K. V.; Lam, Z.; Lau, W. K. O.; Leong, W. K.; Olivo, M. A transition metal carbonyl probe for use in a highly specific and sensitive SERS-based assay for glucose. *J. Am. Chem. Soc.* **2013**, *135*, 18028−18031.
(18) James, T. D.; Sandanayake, K. R. A. S.; Shinkai, S. A Glucose-Selective Molecular Fluorescence Sensor. *Angew. Chem., Int. Ed.* **1994**, *33*, 2207−2209.
(19) Zhao, J.; Fyles, T. M.; James, T. D. Chiral binol-bisboronic acid as fluorescence sensor for sugar acids. *Angew. Chem., Int. Ed.* **2004**, *43*, 3461−3464.
(20) James, T. D.; Sandanayake, K. R. A. S.; Shinkai, S. Saccharide sensing with molecular receptors based on boronic acid. *Angew. Chem., Int. Ed.* **1996**, *35*, 1910−1922.
(21) Eggert, H.; Frederiksen, J.; Morin, C.; Norrild, J. C. A new glucose-selective fluorescent bisboronic acid. First report of strong α-furanose complexation in aqueous solution at physiological pH. *J. Org. Chem.* **1999**, *64*, 3846−3852.
(22) Ancla, C.; Lapeyre, V.; Gosse, I.; Catargi, B.; Ravaine, V. Designed Glucose-Responsive Microgels with Selective Shrinking Behavior. *Langmuir* **2011**, *27*, 12693−12701.
(23) Kong, K. V.; Lam, Z.; Lau, W. K. O.; Leong, W. K.; Olivo, M. A Transition Metal Carbonyl Probe for Use in a Highly Specific and Sensitive SERS-Based Assay for Glucose. *J. Am. Chem. Soc.* **2013**, *135*, 18028−18031.
(24) Schmidt, M. S.; Hübner, J.; Boisen, A. Large Area Fabrication of Leaning Silicon Nanopillars for Surface Enhanced Raman Spectroscopy. *Adv. Mater.* **2012**, *24*, OP11−OP18.
(25) Sun, F.; Bai, T.; Zhang, L.; Ella-Menye, J.-R.; Liu, S.; Nowinski, A. K.; Jiang, S.; Yu, Q. Sensitive and Fast Detection of Fructose in Complex Media via Symmetry Breaking and Signal Amplification Using Surface-Enhanced Raman Spectroscopy. *Anal. Chem.* **2014**, *86*, 2387−2394.
(26) Yetisen, A. K.; Jiang, N.; Fallahi, A.; Montelongo, Y.; Ruiz-Esparza, G. U.; Tamayol, A.; Zhang, Y. S.; Mahmood, I.; Yang, S.-A.; Kim, K. S.; Butt, H.; Khademhosseini, A.; Yun, S.-H. Glucose-Sensitive Hydrogel Optical Fibers Functionalized with Phenylboronic Acid. *Adv. Mater.* **2017**, *29*, 1606380.
(27) Elsherif, M.; Hassan, M. U.; Yetisen, A. K.; Butt, H. Glucose Sensing with Phenylboronic Acid Functionalized Hydrogel-Based Optical Diffusers. *ACS Nano* **2018**, *12*, 2283−2291.
(28) Abikshyeet, P.; Ramesh, V.; Oza, N. Glucose estimation in the salivary secretion of diabetes mellitus patients. *Diabetes, Metab. Syndr. Obes.: Targets Ther.* **2012**, *5*, 149−154.
(29) Campbell, M. J. A. Glucose in the saliva of the non-diabetic and the diabetic patient. *Arch. Oral Biol.* **1965**, *10*, 197−205.
(30) Huang, Y.-J.; Ouyang, W.-J.; Wu, X.; Li, Z.; Fossey, J. S.; James, T. D.; Jiang, Y.-B. Glucose Sensing via Aggregation and the Use of "Knock-Out" Binding To Improve Selectivity. *J. Am. Chem. Soc.* **2013**, *135*, 1700−1703.
(31) Deng, G.; James, T. D.; Shinkai, S. Allosteric Interaction of Metal Ions with Saccharides in a Crowned Diboronic Acid. *J. Am. Chem. Soc.* **1994**, *116*, 4567−4572.
(32) James, T. D.; Sandanayake, K. R. A. S.; Shinkai, S. Recognition of sugars and related compounds by "reading-out"-type interfaces. *Supramol. Chem.* **1995**, *6*, 141−157.
(33) Balan, P.; Babu, S.; Sucheta, K.; Shetty, S.; Rangare, A.; Castelino, R.; Fazil, A. Can saliva offer an advantage in monitoring of diabetes mellitus?—A case control study. *J. Clin. Exp. Dent.* **2014**, *6*, e335−e338.
(34) Jurysta, C.; Bulur, N.; Oguzhan, B.; Satman, I.; Yilmaz, T. M.; Malaisse, W. J.; Sener, A. Salivary Glucose Concentration and Excretion in Normal and Diabetic Subjects. *J. Biomed. Biotechnol.* **2009**, *2009*, 430426.
(35) Gupta, S.; Nayak, M.; Sunitha, J.; Dawar, G.; Sinha, N.; Rallan, N. Correlation of salivary glucose level with blood glucose level in diabetes mellitus. *J. Oral Maxillofac. Pathol.* **2017**, *21*, 334−339.
(36) Tiongco, R. E.; Bituin, A.; Arceo, E.; Rivera, N.; Singian, E. Salivary glucose as a non-invasive biomarker of type 2 diabetes mellitus. *J. Clin. Exp. Dent.* **2018**, *10*, e902−e907.
(37) Naing, C.; Mak, J. W. Salivary glucose in monitoring glycaemia in patients with type 1 diabetes mellitus: a systematic review. *J. Diabetes Metab. Disord.* **2017**, *16*, 2.
(38) Mascarenhas, P.; Fatela, B.; Barahona, I. Effect of Diabetes Mellitus Type 2 on Salivary Glucose—A Systematic Review and Meta-Analysis of Observational Studies. *PLoS One* **2014**, *9*, No. e101706.
(39) Soni, A.; Jha, S. K. Smartphone based non-invasive salivary glucose biosensor. *Anal. Chim. Acta* **2017**, *996*, 54−63.
(40) Mayhall, C. W.; Butler, W. T. The carbohydrate composition of experimental salivary pellicles. *J. Oral Pathol. Med.* **1976**, *5*, 358−370.
(41) He, H.; Xu, X.; Wu, H.; Jin, Y. Enzymatic Plasmonic Engineering of Ag/Au Bimetallic Nanoshells and Their Use for Sensitive Optical Glucose Sensing. *Adv. Mater.* **2012**, *24*, 1736−1740.
(42) Badugu, R.; Lakowicz, J. R.; Geddes, C. D. Noninvasive Continuous Monitoring of Physiological Glucose Using a Monosaccharide-Sensing Contact Lens. *Anal. Chem.* **2004**, *76*, 610−618.
(43) Ma, J.-L.; Yin, B.-C.; Wu, X.; Ye, B.-C. Simple and Cost-Effective Glucose Detection Based on Carbon Nanodots Supported on Silver Nanoparticles. *Anal. Chem.* **2017**, *89*, 1323−1328.
(44) Santos, M. C. D.; Monteiro, J. D.; Araújo, J. M. G.; Lima, K. M. G. Molecular fluorescence spectroscopy with multi-way analysis techniques detects spectral variations distinguishing uninfected serum versus dengue or chikungunya viral infected samples. *Sci. Rep.* **2020**, *10*, 13758.

https://dx.doi.org/10.1021/acssensors.0c02533
ACS Sens. 2021, 6, 1240−1247